TWO-DIMENSIONAL EXTRAPOLATION AND SPECTRAL ESTIMATION FROM ARBITRARY SAMPLING CONFIGURATIONS FOR SAR/ISAR IMAGING.*

Sergio D. Cabrera[1], Benjamin C. Flores[1], Eulalio Rodriguez[1], and Gabriel Thomas[2]

[1]Dept. of Electrical and Computer Eng.
University of Texas at El Paso
El Paso, TX 79968-0523 USA

[2]Engineering and Systems Department
ITESM Campus Chihuahua
31110 Chihuahua, Chih. MEXICO

ABSTRACT[1]

The Adaptive Weighted Norm Extrapolation (AWNE) procedure of Cabrera and Parks is generalized to non-uniform One-Dimensional (1-D) and Two-Dimensional (2-D) sampling configurations. This extrapolation procedure which is based on *iterative modification of the frequency weighting function* in minimum weighted norm extrapolation produces high frequency-domain resolution. The approach presented is derived for totally arbitrary sampling configurations to include those that appear in Inverse Synthetic Aperture Radar (ISAR) imaging of a rotating object. The resulting procedure produces estimates of signal samples on rectangular coordinates in the neighborhood of the given samples (interpolation) as well as beyond (extrapolation). When applied to SAR/ISAR imaging, the procedure produces a complex reflectivity image in the slant-range cross-range domain from the samples of the object's Fourier transform, available at non-cartesian coordinate locations. Examples illustrate the performance of this interpolation/extrapolation procedure using samples of 1-D and 2-D sums of complex sinusoids to simulate range profiles and images of a few point scatterers.

I- INTRODUCTION

The problem of SAR/ISAR imaging often involves polar reformatting of the data samples to produce a set that corresponds to a cartesian raster for subsequent processing with the Discrete Fourier Transform (DFT) [1]. Figure 1 shows the first step in the reformatting for a sampling configuration that result when a rotating object is imaged.

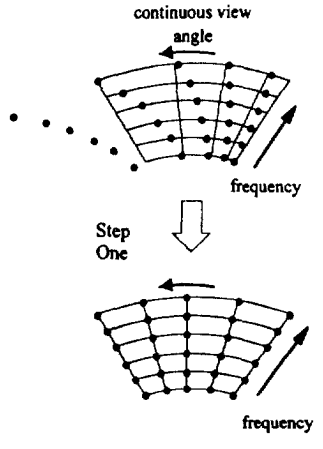

Figure 1: First step in conventional polar reformatting in ISAR imaging of a rotating object with angular acceleration.

[1] *This work was supported in part by the Ballistic Missile Defense Organization as administered by ONR under Contract No. N00014-94-1-0864; by a Patricia Robert Harris Fellowship to E. Rodriguez; and by a Graduate Fellowship to G. Thomas from the Agency for Intl. Development.

This type of procedure can lead to a set of phase history samples covering a total area that is smaller than that of the original data set, and therefore some resolution can be lost.

In radar, the signals that are collected are well modeled as complex sinusoids and therefore imaging procedures that produce high resolution (superresolution) have been considered [2]. The recent interest in superresolution techniques for SAR/ISAR imaging is focused mostly on the use of high-resolution spectrum estimators in their one- and two-dimensional versions. Superresolution is also the result of using *a priori* information about the object to be reconstructed such as the size of the object to be imaged [3].

A well know equivalent problem is bandlimited interpolation/extrapolation in which the signal's spectral support (bandwidth) is known in addition to a *finite* set of samples [4]. This procedure has an optimal solution which is the minimum energy bandlimited signal which goes through the data. It can be used to estimate continuous-time signals from samples located at arbitrary time instants [5], [6]. The two-dimensional case has been addressed in [7]. The bandwidth information can be generalized to the knowledge of the spectral shape of the signal using of a frequency weight function [8], [9].

An iterative procedure to produce and use a data-derived frequency weight function has been developed by Cabrera and Parks which we call here the Adaptive Weighted Norm Extrapolation (AWNE) procedure [9]. The frequency weight is obtained using the periodogram spectrum estimator (using a window and no averaging) applied not only to the given samples but to a larger set of data that includes some values obtained from a previous extrapolation. The procedure can be used for spectrum estimation from short data records to obtain a stationary extension of the data.

This iterative procedure, to be extended in this paper, has been used only on discrete-time signals including sinusoids in noise [10]. For the case in which we have L consecutive samples $\{x(0),x(1),x(2),...,x(L-1)\}$, the procedure has been interpreted as a *nonparametric* , *high-resolution* spectrum estimator that does not require any *a priori* frequency-domain information. More recently, the AWNE method has been evaluated as a method that enhances resolution in time-varying spectrum analysis [11], in SAR image formation by direct phase history extrapolation [12], and in various bilinear time-frequency representations [13]. In this paper, the AWNE procedure is generalized to work with samples taken at arbitrary locations for 1-D and 2-D signals.

II- INTERPOLATION AND EXTRAPOLATION FROM NON-UNIFORM SAMPLES AND *A PRIORI* BANDWIDTH INFORMATION.

A. Conventional Bandlimited Extrapolation from Non-Uniform Samples.

A non-iterative procedure that estimates a signal from given non-uniform samples and known bandwidth [6] is reviewed in this section to establish the theory and notation. A more detailed derivation is given in [14, Chap. 3]. The available

information about the signal is a set of observations $\{x(t_i), i=0,1,...,L-1\}$ from the unknown signal $x(t)$ which has a bandwidth $[-\beta,\beta]$ i.e.,

$$X(f) = \int_{-\infty}^{\infty} x(t) \exp\{-j2\pi ft\}\, dt = 0, \text{ for } |f| > \beta .$$

The energy of $x(t)$ is assumed to be bounded, or $x(t) \in L_2(-\infty,\infty)$. The chosen extrapolation $x_{BL}(t)$ will meet the minimal requirements of having bandwidth $[-\beta,\beta]$ and being consistent with the samples, i.e., $x_{BL}(t_i)=x(t_i)$ for $i=0,1,...,L-1$.

The standard inner product can be used to define a Hilbert space of bandlimited signals in $L_2(-\infty,\infty)$ so that the sample $x(t_i)$ can be expressed as the bounded linear mapping

$$f_i(x) = (x\,,\, \phi_i) = x(t_i)$$

with the sampling functions equal to

$$\phi_i(t) = s(t-t_i) = \frac{\sin 2\pi\beta(t-t_i)}{\pi(t-t_i)} \qquad (1)$$

It is also not difficult to prove that all the sampling functions are linearly independent if and only if all the sampling instants are distinct.

There are infinitely many solutions which satisfy the requirement of both sample consistency and spectral support. The minimum norm solution can be easily shown to be in the subspace spanned by the L sampling functions, i.e.,

$$x_{BL}(t) = \sum_{i=0}^{L-1} \alpha_i\, s(t-t_i) \qquad (2)$$

To see this we note that any signal $y(t)$ in the orthogonal complement of this subspace can be added to $x_{BL}(t)$ to give another valid solution with larger energy since $y(t_i)=0$; $i=0,1,2,...,L-1$.

The extrapolation coefficients (α_i's) can be solved for from the matrix equation that provides a valid extrapolation:

$$\begin{bmatrix} s(t_0-t_0) & s(t_0-t_1) & \cdots & s(t_0-t_{L-1}) \\ s(t_1-t_0) & s(t_1-t_1) & \cdots & s(t_1-t_{L-1}) \\ \vdots & \vdots & \cdots & \vdots \\ s(t_{L-1}-t_0) & \cdots & \cdots & s(t_{L-1}-t_{L-1}) \end{bmatrix} \begin{bmatrix} \alpha_0 \\ \alpha_1 \\ \vdots \\ \alpha_{L-1} \end{bmatrix} = \begin{bmatrix} x(t_0) \\ x(t_1) \\ \vdots \\ x(t_{L-1}) \end{bmatrix} \qquad (3)$$

In matrix/vector notation $\mathbf{G}\underline{\alpha} = \underline{y}$. It is not difficult to show that the Gram matrix $\mathbf{G}$ is non-singular for distinct sampling instants (which we assume here) and therefore $\underline{\alpha} = \mathbf{G}^{-1}\,\underline{y}$.

B. Signal extrapolation with energy concentration information in the frequency domain.

Suppose that in the above problem, we also have *a priori* information about the distribution of signal energy in the frequency domain. This can be in the form of a weight function $Q(f)>0$ for $|f|<\beta$, and, $Q(f) = 0$ for $|f|>\beta$. This can can be used to improve the result by finding a bandlimited extrapolation which has a spectral shape closely resembling $Q(f)$. The desired estimate of $x(t)$ can be obtained by minimizing a frequency weighted norm of the form:

$$\|x\|_Q^2 = (x\,,x)_Q = \int_{-\beta}^{\beta} \frac{1}{Q(f)} X(f)\, X^*(f)\, df$$

to get the desire extrapolation which we denote $x_Q(t)$. With the weighted inner product that leads to this norm, the samples can be expressed as

$$x(t_i) = \int_{-\beta}^{\beta} X(f)\exp(j2\pi ft_i)df = \int_{-\beta}^{\beta} \frac{X(f)}{Q(f)}[Q(f)\exp(-j2\pi ft_i)]^* df$$
$$= (\,x(t)\,,\, q(t-t_i)\,)_Q$$

where $q(t)$ is the inverse Fourier transform of $Q(f)$. Now, the result is the minimum weighted norm extrapolation

$$\hat{x}_Q(t) = \sum_{i=0}^{L-1} \alpha_i\, q(t-t_i) \qquad (4)$$

which requires that we solve the following linear equations:

$$\begin{bmatrix} q(t_0-t_0) & q(t_0-t_1) & \cdots & q(t_0-t_{L-1}) \\ q(t_1-t_0) & q(t_1-t_1) & \cdots & q(t_1-t_{L-1}) \\ \vdots & \vdots & \cdots & \vdots \\ q(t_{L-1}-t_0) & \cdots & \cdots & q(t_{L-1}-t_{L-1}) \end{bmatrix} \begin{bmatrix} \alpha_0 \\ \alpha_1 \\ \vdots \\ \alpha_{L-1} \end{bmatrix} = \begin{bmatrix} x(t_0) \\ x(t_1) \\ \vdots \\ x(t_{L-1}) \end{bmatrix}.$$

III- THE ADAPTIVE WEIGHTED NORM EXTRAPOLATION PROCEDURE FOR NON-UNIFORM SAMPLES.

The procedures discussed in Sect. II can give interpolation/extrapolation from non-uniform samples making optimal use of the *a priori* information about bandwidth or frequency-domain energy concentration. In SAR/ISAR imaging, there is an interest in exploiting the nature of the radar return signals to obtain higher than conventional resolution in computing profiles (1-D) or images (2-D).

A. Procedure to produce high frequency-domain resolution.

The two approaches of Sect. II can be combined to formulate a procedure which gives high frequency-domain resolution. The rationale for the procedure is that in addition to using *a priori* bandwidth information, it is possible to derive a useful frequency weight $Q(f)$ (for use in minimum weighted norm extrapolation) from the data itself [9]. Clearly a spectrum estimator can provide such a quantity from the samples. Therefore, an iterative procedure can be formulated to generate $Q(f)$ from the spectrum of the previous extrapolation so that even higher resolution can be obtained. This idea has already proven to be very useful using only time-domain samples of discrete-time signals [9]. In this section, we illustrate the procedure for data corresponding to known non-uniform sample locations for continuous-time signals.

Let us assume that $x(t)$ is the desired signal to interpolate/extrapolate and that it has a bandwidth $[-\beta,\beta]$ (or a more general spectral support region with indicator function $B(f)$). From Sect. II, the resulting minimum energy, bandlimited extrapolation has the form given by Eqs. (1)-(3). The resulting signal is the best possible recovery of $x(t)$ from the available information in the sense of minmax worst case error in the estimation of any linear transformation derived from $x(t)$, including $x(t)$ itself [9]. The resulting signal $\hat{x}_{BL}(t)$ has a spectrum with low resolution since it has minimal energy and is therefore concentrated in the time domain near the locations of the given samples $\{t_0<t_1<...<t_{L-1}\}$. This spectrum is an optimal estimate of that of the true signal $x(t)$ when no other information about the signal is used.

If we know that the signal has a narrowband spectrum, this first estimate can be used to define a weighting function $Q_2(f)$ to obtain a less time-concentrated extrapolation having a spectrum that is more concentrated. This refinement procedure can be repeated more than once in an iterative way. To formalize, we define the first iteration assuming a spectral support indicator function $B(f)$ as:

$$Q_1(f) = B(f) \; ; \; \hat{x}_1(t) = \hat{x}_{BL}(t) \; .$$

The Q(f) for the second iteration can be defined as a sidelobe-reduced version of the spectrum of $\hat{x}_1(t)$ which requires the use of a time-domain window. The use of a fixed size window at each iteration also makes the iterative procedure converge to a fixed solution by limiting the growth of q(t) to a maximum length. From Eq. (4) we see that this will limit the length of the extrapolation to a maximum. Following these ideas we therefore define:

$$\tilde{x}_1(t) = \hat{x}_1(t) \cdot p(t)$$

where p(t) is a standard window such as a Hamming window.

The second frequency weight $Q_2(f)$ is therefore equal to a modified periodogram [15] computed from the first extrapolation. The second extrapolation is then the minimum weighted norm solution using this new frequency weight. Using this idea more than twice leads to an iterative algorithm illustrated in Fig. 1. The updating equations assuming a spectral support indicator function B(f) are given as:

$$\tilde{x}_k(t) = \hat{x}_k(t)\; p(t) \qquad ; \; \hat{x}_{k+1}(t) = \sum_{i=0}^{L-1} \alpha_i^{(k+1)} q_{k+1}(t - t_i)$$

$$Q_{k+1}(f) = |\tilde{X}_k(f)|^2 \; B(f)$$

We note that this procedure uses a frequency weighting function $Q_k(f)$ that depends on the given data for k≥2, and therefore we consider it to be "adaptive." In a practical implementation of this algorithm, it is necessary to evaluate $\hat{x}_k(t)$ on a grid $t=nT_o$ with T_o small enough. In doing this at each iteration, it is necessary to numerically interpolate to obtain $q_k(t)$ at various non-uniformly spaced locations such as:

$$q_k(nT_o - t_i) \; ; \; q_k(t_j - t_m) \; ; \; 0 \le i,j,m \le L\text{-}1$$

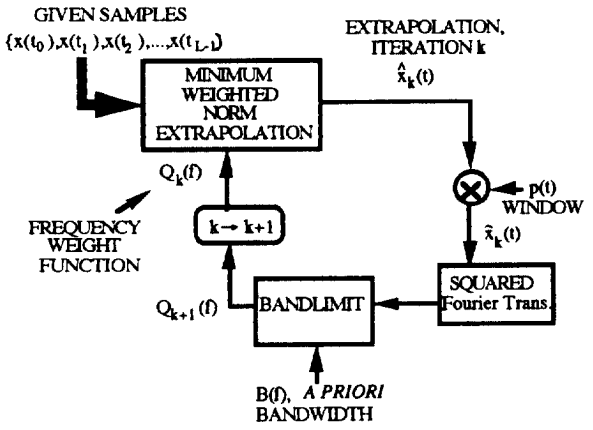

Figure 2: The Adaptive Weighted Norm Extrapolation (AWNE) Algorithm for Continuous-Time signals using Non-Uniformly Sampled Data.

B. Examples of 1-D non-uniform interpolation/ extrapolation with high resolution.

We consider a test signal which is suitable for evaluation of this method for calculation of one-dimensional radar profiles. The signal used is a sum of two complex sinusoids of the form

$$x(t) = A_1 \, e^{j2\pi(f_1 t + \phi_1)} + A_2 \, e^{j2\pi(f_2 t + \phi_2)}$$

$$A_1=A_2=1.0 \; ; \; f_1 = 0.27 \; ; \; f_2 = 0.29 \; ; \; \phi_1 = 0.0 \; ; \; \phi_2 = \frac{\pi}{4}$$

This test signal's real part is shown in Fig. 3 in the range [1,256]. For test purposes, we generate a set of L=33 non-uniformly spaced sampling instants starting at t_0=100 using a random number generator to get the spacings Δ_k so that:

$$t_{k+1} = t_k + \Delta_k \; ; \; k=0,1,2,...,L\text{-}2$$

with the Δ_k's chosen to have an equally likely value in the interval [0.2,2.0]. The real part of the samples at these locations are shown on the next graph in Fig. 3.

Noting that the above signal is band-pass in nature, we select a spectral support region of the form $[B_1,B_2]$ where B_1=0.0 and B_2=0.6 cycles/sample. A Hamming window p(t) of length 65 is used to smooth the spectra between iterations so as to limit the extrapolation length at each iteration to the range $[t_0$-64,t_{L-1}+64] or [36,197]. The AWNE procedure is executed for 5 iterations during which convergence is achieved. The results of the first iteration (bandlimited extrapolation) are shown in the next graph in Fig. 3 and is clearly unsatisfactory for many applications. After 5 iterations we obtain a less concentrated signal (with approximately 3 times as much energy) shown in the next plot. The magnitude spectra for these two signals are shown in the last two plots in Fig. 3.

This example shows that using the AWNE approach we obtain an extrapolation with a spectrum that very accurately represents the signal used to obtain the data. For example, the two accurately located peaks in the spectrum of iteration No. 5 correctly exhibit equal height. In addition, due to the naturally tapered nature of the extrapolation, little sidelobe effects are visible in this spectrum.

IV- TWO-DIMENSIONAL NON-UNIFORM SAMPLING CONFIGURATIONS IN ISAR IMAGING.

In this section, we will discuss the types of non-uniform sampling configuration encountered in stepped-frequency ISAR, in which an object of finite extent is imaged by taking advantage of its rotating motion relative to the radar platform. In this section we also discuss the conventional procedure of polar reformatting which seeks only to interpolate and not to extrapolate.

Stepped-frequency ISAR is a radar imaging technique that maps the reflectivity of an object into a two-dimensional plane [16] with coordinates referred to as slant range "r" and cross range "s". Ordinarily, slant range information is obtained by processing the echoes of a series of pulse trains (bursts) into a history of slant range profiles. Each of these is generated by first obtaining a set of baseband complex samples from the echoes of each stepped-frequency burst. For a fully illuminated object located in the far field, the samples represent the frequency response of the object.

Performing the Inverse DFT on the samples yields a complex profile in which spatial characteristics are made discernible in slant range. To extract spatial characteristic in cross range, the complex reflectivity of each slant range is first recorded in time and then processed via the DFT. In effect, this process is equivalent to processing several Doppler cycles in each slant range cell to separate Doppler components. Since Doppler and cross range are linearly related, this procedure leads to a complete mapping of the object's reflectivity in two spatial dimensions.

The premise of ISAR imaging is that in effect there is a relative rotational motion between the object and the radar platform. This motion can either be discrete or continuous. Discrete rotational motion is encountered only in controlled environments, i.e. experimental radar ranges and anechoic chambers. In this instance, the echo samples are arranged in a polar raster with coordinates (f_i,θ_j) given by

$$f_i=f_o+ i\,\Delta f \; ; \; i=0,1,...n\text{-}1 \; ; \; \theta_j=\theta_o+ j\,\delta\theta \; ; \; j=0,1,...,m\text{-}1,$$

where f_o is the initial frequency, Δf is the frequency step between adjacent pulses in a burst, θ_o is the initial viewing angle, and $\delta\theta$ is the discrete angular change. It follows that the frequency step and the angular change can be calculated as $\Delta f = \beta/(n-1)$ and $\delta\theta = \Delta\theta/(m-1)$, where β is the frequency bandwidth spanned by each burst and $\Delta\theta$ is the total aspect change associated with the synthetic aperture.

In contrast to discrete motion, continuous motion occurs in scenarios were objects engage in real world maneuvers. Here the echo samples are assigned polar coordinates (f,θ) where both f and θ are parametric expressions of time. Specifically, the pulse frequency f is given by

$$f(t_{ij}) = f_o + \beta\frac{(t_{ij} - njT_2)}{(n-1)T_2} \; ; \; t_{ij} = (i + nj)T_2$$

where i=0,1,...,n-1, and j=0,1,...m-1. Here T_2 is the pulse repetition interval as well as the sampling interval. Clearly, the frequency sweep is discrete with a period of nT_2 seconds. As for the viewing angle θ, its general expression is a polynomial in time

$$\theta(t_{ij}) = \theta_o + \Omega\, t_{ij} + \frac{1}{2}\alpha\, t_{ij}^2 + \ldots$$

where Ω is the initial angular rate of rotation, α is the angular acceleration. Higher order terms such as the angular jerk can be included as needed.

For this motion model, the aspect change is $\Delta\theta=\Omega T + 1/2\alpha T^2$ where the total (coherent) integration time T is $(nm-1)T_2$ Under the condition that the aspect change $\Delta\theta<<1$ rad. and that $\beta/f_o<0.1$, the image resolutions in slant range and cross range are respectively $\Delta r=c/2\,\beta$ and $\Delta s=\lambda/2\Delta\theta$, where λ is the wavelength at midband.

The above conditions represent the specific case of focused ISAR. For wider aspect changes, the focused area on the image plane is limited to a blur radius r_b. This effect is caused by the migration of individual scatterers through one or more image cells during the integration time. Cell migration results from the fact that the samples on the f-θ plane are collected and processed while the object rotates, causing a deviation from cartesian coordinates.

The classical solution to the problem of sampling over a wide synthetic aperture is polar reformatting [1] in which samples are interpolated to obtain samples on the desired coordinates

$$f_r = f\cos(\theta) \; ; \; f_s = f\sin(\theta) \; .$$

A conventional polar reformatting procedure results in interpolated samples in a region contained exclusively within the area of the available samples. In the case of discrete rotation, only two steps are required [16], the first one being a sequence of frequency interpolations for each viewing angle to achieve uniform spacing in the f_r direction. The second step is a sequence of interpolations along the f_s direction, providing uniform spacing which can then be processed into an ISAR image using the 2-D DFT.

In the case of continuous motion, three steps are required [17]. The first step shown in Fig. 1 involves an angular interpolation for each frequency step to yield samples on a polar grid. Since this is configuration is identical to that of the discrete rotation case, the remaining two steps are identical to the reformatting for that case.

In both of the above cases, the interpolation of samples must be performed at equal intervals in f_r and f_s over a reduced region of bandwidths β_r and β_s. The desired spacings within this region are [18]

$$\Delta f_r = \beta_r/(n-1) = (f_{n-1}\cos(\Delta\theta/2) - f_o)/(n-1) \; ;$$

$$\Delta f_s = \beta_s/(m-1) = (2f_o\tan(\Delta\theta/2))/(m-1) \; .$$

Upon resampling, the new coordinates are given by $f_{ri}=f_o+ i\,\Delta f_r$ and $f_{sj}=-f_o\tan(\Delta\theta/2) + j\,\Delta f_s$. The following change of variables leads to more significant set of spatial frequency coordinates:

$$R = 2f_r/c = 2f\cos(\theta)/c \; ; \; S = 2f_s/c = 2f\sin(\theta)/c \; .$$

For an object g(r,s) with Fourier transform G(R,S), the units for R and S are m^{-1} [1]. The corresponding bandwidths are given as $\Delta R = 2\,\beta_r/c$ and $\Delta S = 2\,\beta_s/c$.

It follows that for a signal collected over a region of area $\Delta R\Delta S$ in the (R-S) plane, the resolution in slant range is $\Delta r=1/\Delta R$ while the resolution in cross range is $\Delta s=1/\Delta S$. The normalized units R and S will be used in the next section for an object support region A in the (r-s) plane which is fully contained in a normalized square with each side measuring 1 m. By the Nyquist sampling criterion, the spacing between samples in the (R-S) domain must be less than one.

V- EXTENSION OF THE ADAPTIVE WEIGHTED NORM EXTRAPOLATION METHOD TO 2-D NON-UNIFORM SAMPLING CONFIGURATIONS.

A. Estimation of the reflectivity of a rotating object from non-uniformly spaced Fourier transform values.

The procedure described in sections II and III can be easily extended to the 2-D ISAR Fourier inversion problem including the limited support constraint in the (r-s) spatial domain. The notation used for the signal in question is g(r,s) and its Fourier transform is:

$$G(R,S) = \int_{-\infty}^{\infty}\int_{-\infty}^{\infty} g(r,s)\,\exp\{-j2\pi(Rr + Ss)\}\,dr\,ds$$

We assume that the object is of limited size so that g(r,s)=0 for $(r,s)\notin A$. The extension is simplest if the arbitrary locations and values of the two-dimensional Fourier transform of the object are ordered to form a one-dimensional list $\{G(R_i,S_i);\ i=0,1,2,3,\ldots,L-1\}$.

The indicator function for the region A in the (r-s) plane is $b_A(r,s)$ and its Fourier transform is $B_A(R,S)$ so that $g(r,s)=b_A(r,s)g(r,s)$. The sampling functions are $B_A(R-R_i,S-S_i)$ since each sample is given as an (r-s) domain inner-product of the form:

$$G(R_i, S_i) = \int_{-\infty}^{\infty}\int_{-\infty}^{\infty} g(r,s)\,(b_A(r,s)\,\exp\{j2\pi(rR_i+sS_i)\})^*\,dr\,ds$$

The minimum energy 2-D bandlimited extrapolation now takes the form:

$$G_{BL}(R,S) = \sum_{i=0}^{L-1} \alpha_i\, B_A(R-R_i\,,\,S-S_i)$$

which requires solving the following equations:

$$\begin{bmatrix} B_A(R_0-R_0,S_0-S_0) & B_A(R_0-R_1,S_0-S_1) & \cdots & B_A(R_0-R_{L-1},\ldots) \\ B_A(R_1-R_0,S_1-S_0) & B_A(R_1-R_1,S_1-S_1) & \cdots & B_A(R_1-R_{L-1},\ldots) \\ \vdots & \vdots & \ddots & \vdots \\ B_A(R_{L-1}-R_0,\ldots) & \cdots & \cdots & B_A(0,0) \end{bmatrix} \begin{bmatrix} \alpha_0 \\ \alpha_1 \\ \vdots \\ \alpha_{L-1} \end{bmatrix} = \begin{bmatrix} G(R_0,S_0) \\ G(R_1,S_1) \\ \vdots \\ G(R_{L-1},S_{L-1}) \end{bmatrix}$$

The case of weighted norm extrapolation with object support information makes use of a frequency weight q(r,s)>0 for $(r,s)\in A$ and q(r,s)=0 for $(r,s)\notin A$. The equations for this case

are identical to those indicated above with $B_A(R,S)$ replaced by $Q(R,S)$, the Fourier transform of $q(r,s)$. The extension of the iterative AWNE procedure to the two-dimensional case is also straight forward since all the components of the algorithm, including the windowing operation, have a 2-D counterpart.

B. Examples of 2-D Extrapolation from Non-Uniform Samples.

We consider a test signal which is suitable for evaluation of expected performance of these methods in ISAR imaging. The test signal used consists of two impulse targets at (r_1,s_1) and (r_2,s_2) which produce a Fourier transform equal to a sum of two complex sinusoids of the form:

$$G(R,S) = A_1 e^{-j2\pi(r_1R+ s_1S)} + A_2 e^{-j2\pi(r_2R+ s_2S)}$$

$$A_1=A_2=1.0 \; ; \; r_1=s_1=0.2 \; ; \; r_2=s_2=0.3$$

For test purposes we will use $L=16^2$ samples in the (R-S) plane, configured as shown in Fig. 4, to simulate the samples obtained from a continuously rotating object with non-zero angular acceleration. The range of the sample locations is 12 to 28 in each direction (R and S). We select a valid object support region of the form:

$$A= \{(r,s): \; 0\le r \le 0.5 \; ; \; 0\le s \le 0.5\} \; .$$

and the Fourier transform of the object is extrapolated to the range [1-32] in each variable R and S (not shown). Finally, we compute a two-dimensional DFT magnitude to obtain the desired image. Three iterations of AWNE are performed using a fixed length, separable Hamming window of size 15 by 15 roughly equal in size to the square that contains all the given Fourier transform samples in Fig. 4. With such a short window, the AWNE procedure converges quickly in 3 iterations.

The results are shown in the remaining plots of Fig. 4. All results indicate an set of 32 by 32 samples of the image corresponding to the normalized square in the spatial domain. The two contour plots in Fig. 4 show the reconstructed object at the first iteration (bandlimited extrapolation result) and at the third iteration. A mesh plot of the image from iteration No. 1 is also shown on the bottom left. From this image, a weight $q(r,s)$ is defined for use in the second iteration which is the next mesh plot. The final resulting image of iteration No. 3 is the mesh plot at the bottom right.

Clearly the results show a very significant advantage to the use of weighting function refinement (iteration No. 1 vs. No. 3). The reconstructed object at iteration No. 3 clearly shows the correct locations of the peaks and no significant sidelobe structure.

VI- CONCLUSIONS AND FUTURE WORK.

The technique presented in this paper works well for interpolation and extrapolation of complex sinusoids in 1-D and 2-D cases. Therefore, the method appears to be promising in deriving high-resolution radar profiles and reflectivity images directly from non-uniformly spaced data. That is, the technique provides both interpolation and extrapolation of the given samples. We note however that to do this we must have accurate knowledge of the sample locations. In addition, the procedure in its present form is computationally intensive since it requires the calculation of a matrix inversion step at each iteration.

Our future research will include deriving fast algorithms to avoid doing the matrix inversion. We will also evaluate the quality of the reconstruction in the presence of noise and using real ISAR data. Another key goal of our research is to incorporate this procedure within a Motion Compensation scheme to estimate and compensate for unknown object motion. We will also evaluate the sensitivity of the results to errors in the sample locations. Finally, we will evaluate the performance obtained using object support regions that reflect real world scenarios.

VII- REFERENCES.

[1] D. L. Mensa, High-Resolution Radar Cross-Section Imaging, Artech House, 1991.

[2] Stuart R. DeGraaf, "SAR Imaging via Modern 2-D Spectral Estimation Methods," in Algorithms for Synthetic Aperture Radar Imagery, SPIE Vol. 2230, pp. 36-46, April 1994, Orlando, FL.

[3] H. Stark, Ed., Image Recovery: Theory and Application, Academic Press Inc., 1987.

[4] P. J. S. G. Ferreira, "Interpolation and the Discrete Papoulis-Gerchberg Algorithm," IEEE Trans. on Signal Processing, Vol. 42, No. 10, pp. 2596-2606 Oct. 1994.

[5] M. Soumekh, "Band-limited interpolation from unevenly spaced sampled data," IEEE Trans. on Acoustics Speech and Signal Processing, Vol. 36, No. 1, pp. 110-122, Jan. 1988.

[6] G. Calvagno and D. C. Munson, Jr., "New Results on Yen's Approach to Interpolation from nonuniformly spaced samples," in Proc. of ICASSP, April 1990, pp. 1525-1538.

[7] D. S. Chen and J. P. Allebach, "Analysis of Error in Reconstruction of Two-Dimensional Signals from Irregularly Spaced Samples," IEEE Trans. on Acoustics Speech and Signal Processing, Vol. 35, No. 2, pp. 173-180, Feb. 1987.

[8] L. C. Potter and K. S. Arun, "Energy Concentration in Band-Limited Extrapolation", IEEE Trans. ASSP, Vol. ASSP-37, pp.1027-1041, July 1989.

[9] S. D. Cabrera and T. W. Parks, "Extrapolation and Spectral Estimation with Iterative Weighted Norm Modification", IEEE Trans. on Signal Processing, Vol. 39, No. 4, pp. 842-851, April 1991.

[10] S. D. Cabrera, J. T. Yang and C. Chi, "Improved Approaches to Estimation of Sinusoids by Adaptive Band-Limited Extrapolation," Proc. of Fifth ASSP Workshop on Spectrum Estimation and Modeling, Rochester NY, pp. 35-39, Oct. 1990.

[11] S. D. Cabrera, B. C. Flores, G. Thomas and J. Vega-Pineda, "Evolutionary Spectral Estimation Based on Adaptive Use of Weighted Norms", SPIE Vol. 2027, pp. 168-179, July 1993, San Diego, CA.

[12] S. D. Cabrera, B. C. Flores, G. Thomas and J. Vega-Pineda, "Applications of One-Dimensional Adaptive Extrapolation to Improve Resolution in Range-Doppler Imaging", SPIE Vol. 2230, pp. 135-145, April 1994.

[13] G. Thomas, and S. D. Cabrera, "Resolution Enhancement in Time-Frequency Distributions Based on Adaptive Time Extrapolations," Proc. of IEEE-SP Intl. Symposium on Time-Frequency and Time-Scale Analysis, pp. 104-107, Philadelphia, PA, Oct. 25-28, 1994.

[14] J. T. Yang, Extrapolation and Spectral Estimation for Sinusoids in Noise, Including A Priori Information, Ph. D. dissertation supervised by S. D. Cabrera, Dept. of Electrical and Computer Engineering, Pennsylvania State Univ., Dec. 1992.

[15] S. L. Marple, Digital Spectrum Analysis with Applications, Prentice-Hall, 1987.

[16] D. R. Wehner, High Resolution Radar, Artech House, Norwood, MA, 1987.

[17] A. Ugarte, An Autonomous Approach to Motion Estimation and Compensation in Range-Doppler Imagery, M. S. Thesis supervised by B. Flores, U. of Texas at El Paso, June 1993.

[18] B. C. Flores, "A Robust Method for the Motion Compensation of ISAR Imagery," SPIE Proc., Vol. 1607, pp. 512-517, 1992.

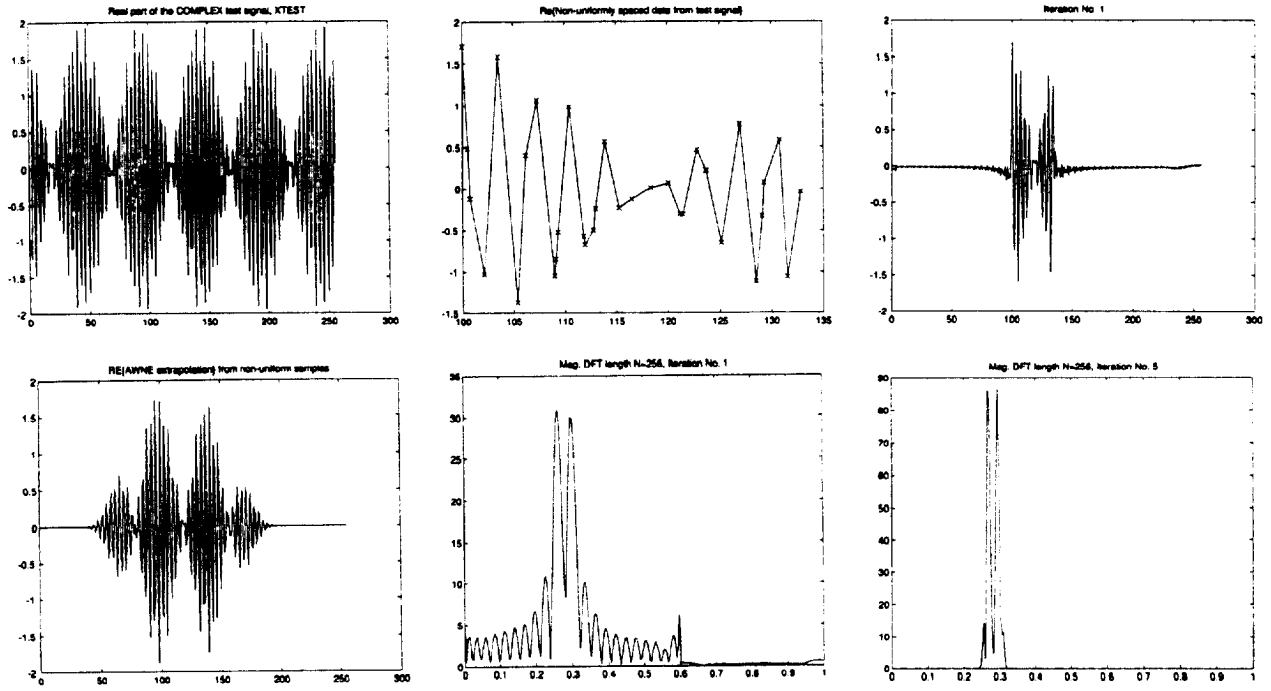

Figure 3. One-Dimensional Example (from left to right & top to bottom): Real part of the test signal; Real part of the non-uniformly spaced samples used to do interpolation/extrapolation; Real part of the extrapolated signal after iteration No. 1 (bandlimited extrapolation); Real part of the result of AWNE after 5 iterations; DFT magnitude of the result of iteration No. 1; DFT magnitude of the result of iteration No. 5.

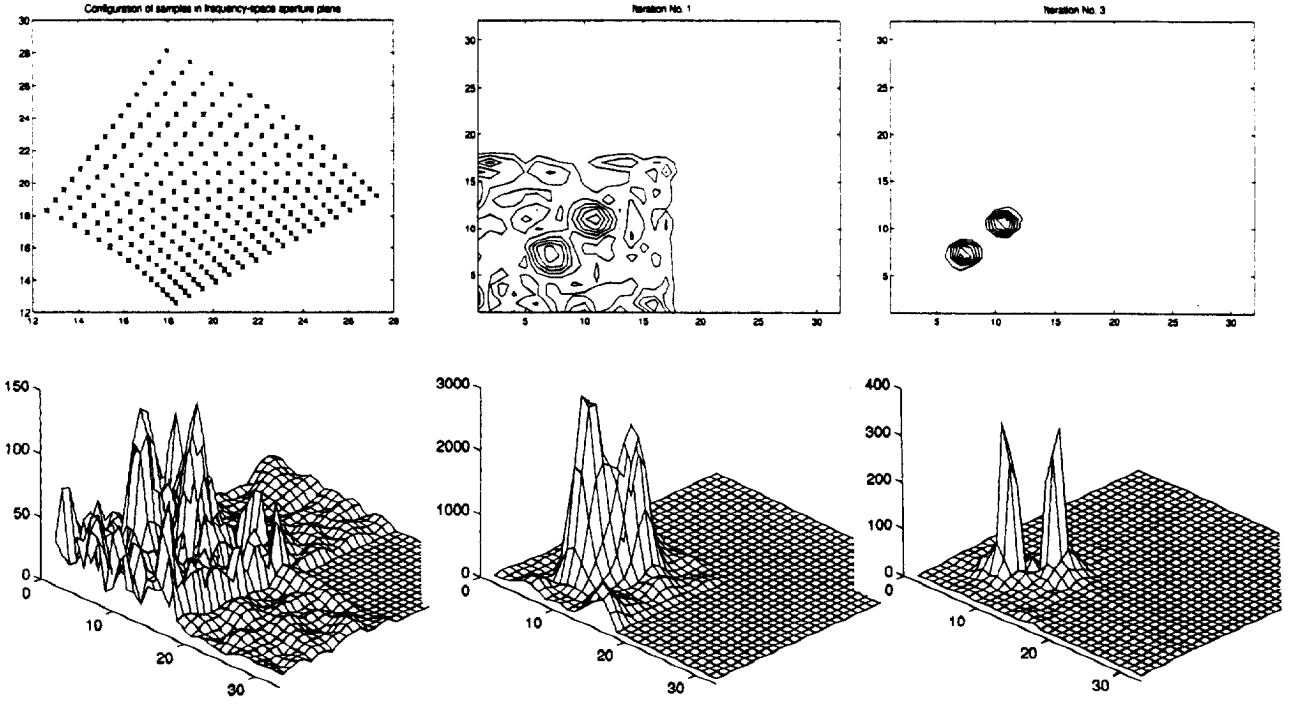

Figure 4. Two-Dimensional Example (from left to right & top to bottom): Configuration of available samples; Contour plot of the resulting image after iteration No. 1; Contour plot of the resulting image after iteration No. 3; Mesh plot of the resulting image after iteration No. 1; Weighting function derived from the result of iteration No. 1 to be used in iteration No. 2; Mesh plot of the resulting image after iteration No. 3.